Journal of Hazardous Materials 195 (2011) 432–439

Contents lists available at SciVerse ScienceDirect

Journal of Hazardous Materials

journal homepage: www.elsevier.com/locate/jhazmat

Can bubble columns be an alternative to fibrous filters for nanoparticles collection?

A. Charvet[a,b,*], N. Bardin-Monnier[a,b], D. Thomas[a,b]

[a] CNRS, Laboratoire Réactions et Génie des Procédés (LRGP), UPR 3349, 1 rue Grandville BP 20451, 54001 Nancy, France
[b] Nancy-Université, UHP, LRGP, 54000 Nancy, France

ARTICLE INFO

Article history:
Received 19 July 2011
Received in revised form 24 August 2011
Accepted 25 August 2011
Available online 31 August 2011

Keywords:
Bubble column
Collection
Nanoparticles

ABSTRACT

The most effective and widely used dedusting techniques to separate nanoparticles of a carrier fluid are fibrous media. The main problem is the clogging of the filter that induces a pressure drop increase over time and thus requires a regular cleaning of the media (or its replacement). Following these observations, this study proposes to investigate the potential of bubble columns for nanoparticles collection. Despite collection efficiencies lower than those of fibrous filters, experimental results show that bubble columns present likely performances for the collection of nanoparticles and have collection efficiency even more important when the liquid height is high and bubbling orifices have low diameters. Experiments have also revealed the presence of a most penetrating particle size for a particle diameter range between 10 and 30 nm. The model developed in this article highlights a good agreement between the theoretical collection efficiency by Brownian diffusion and experimental collection efficiencies for particles lower than 20 nm. Nevertheless, the modelling may be extended to other collection mechanisms in order to explain the collection efficiency increase for particles higher than 20 nm and to confirm or infirm that electrostatic effects can be the cause of this efficiency increase.

1. Introduction

Nanometric aerosols localized in workplace environments mainly stem from two sources: on the one hand, nanoparticles are manufactured in more and more industrial applications and on the other hand, nanoparticles are generated by different processes: fumes, oil mists and metallization. The latter technique, which involves projecting (by compressed air) fine metallic particles on a surface, is a very productive source of ultrafine toxic particles. Indeed, the metals most commonly used are zinc, tin and Zn/Al alloys. Coatings based on most dangerous metals as chromium or nickel are also employed [1]. Ultrafine particle emissions in the environment are increasingly regulated and the appearance of limit values imposes to act on the particle rejections. Currently, the most effective and widely used dedusting techniques to separate nanoparticles of a carrier fluid are fibrous media (often cartridges). These very high efficiency filters are mainly constituted of micron-sized fibres. The main problem with the filtration of such particles is the rapid clogging of the filter. This clogging induces a fast pressure drop increase over time and thus requires a regular cleaning of the media or its replacement. Despite their widespread presence, there is still a lack of models able to predict the time evolution of the pressure drop and the lifetime of such filters and as a consequence these devices are not optimized yet. Moreover, the dust unclogging may be the cause of many problems affecting the performance of filters like a possible re-suspension of nanoparticles previously collected by the media [2,3]. This operation can also induce a deterioration of the filter structure which causes leaks and consequently a severe decrease of filtration efficiency [4]. This media cleaning may thus run counter to the general objective of process and individual safety. The problem is most pronounced in the case of metallization processes as particle concentrations are very high (10^9 particles per cubic centimetre [1]). As a guide, the particle concentration of a polluted environment as can be found near dense road traffic is one thousand times less. In addition, the number size distribution of particles emitted by metallization processes exhibits a population of ultrafine particles (more than 95% of particles of diameter < 100 nm). Nanoparticles tend to form agglomerates which favour the filter clogging. Following these observations, this study proposes to investigate the potential of other dedusting methods that could be applied to metallization fumes. The idea is to test wet scrubbers as an alternative to fibrous filters. One advantage of these separators is that they operate at constant pressure drop and consequently, do not require dust unloading and therefore do not present any risk of nanoparticles re-suspension. This study examines the relevance of wet

* Corresponding author at: CNRS, Laboratoire Réactions et Génie des Procédés (LRGP), UPR 3349, 1 rue Grandville BP 20451, 54001 Nancy, France.
Tel.: +33 0 3 83 17 53 33.
E-mail address: augustin.charvet@ensic.inpl-nancy.fr (A. Charvet).

0304-3894/$ – see front matter © 2011 Elsevier B.V. All rights reserved.
doi:10.1016/j.jhazmat.2011.08.064

scrubbers in terms of collection efficiency and more precisely, the absorption of nanoparticles by bubbling through a liquid will be investigated.

2. Background

A survey of the literature revealed that different wet scrubbers, and in particular bubble and spray columns, have been used for collecting particles from gas streams. Bubble columns offer many advantages such as little maintenance requirement due to simple construction, easy temperature control and low initial costs of installation. However, few studies on scrubbing of particles have been reported. Meikap and Biswas [5] studied the performance of a bubble column with a diameter of 0.19 m and a height of 2 m. The gas velocities were selected to generate bubbles in the size range of 2–5 mm (determined by visual observations). The collection efficiencies for particle sizes between 2 and 50 μm were relatively large (above 97%) and the performance of the wet scrubber increased with the gas flow and the particle concentration entering the column. Moreover, the authors showed that, between 0.2 and 1.3 m, a higher liquid level in the bubble column induced an increase in particle collection. This least observation confirms that of Bandyopadhyay and Biswas [6] who studied the performance of a bubble column for the simultaneous treatment of SO_2 and submicron particles (soot and ash with median diameters of 1.4 and 9.8 μm, respectively). Yuu et al. [7] studied the absorption of submicron particles (with diameters between 1.5 and 3.2 μm) when they are bubbled through water. They showed that the particle capture is almost totally explainable by the mechanism of impaction. They also highlighted that particles are collected with extremely small values of inertia parameter in bubble dust collection compared with fibrous media collection. Nevertheless, bubbling has low collection efficiency compared with other methods such as bag filters. Finally, they emphasized that the collection efficiency increased exponentially with the water height and consequently with the residence time. More recently, Hermeling and Weber [8] studied the collection of carbon nanoparticles by bubbling through different liquids. These authors highlighted that an addition of surfactant in the liquid induces a decrease in bubble size and hence an increase in collection efficiency of nanoparticles. They also observed that the collection efficiency increased exponentially with the liquid level in the bubble column and that an increase in particle size resulted in a decrease in collection efficiency (efficiency of about 95%, 60% and 50% for particles of 18, 55 and 170 nm, respectively). The authors concluded that these results demonstrated the predominance of the diffusion mechanism in the collection of nanoparticles by bubbling through a liquid.

The first theory of absorption of particles in gas bubbles during their rise through a liquid has been developed by Fuchs [9]. Indeed, particles transported in a stable rising bubble may be collected by the surrounding liquid due to different deposition mechanisms. The most predominant ones are Brownian diffusion, inertial deposition and gravitational settling. In his theory, Fuchs characterizes each mechanism of absorption thanks to a corresponding coefficient and considers that each of them depends on the rising velocity of the bubble and consequently on the bubble size, the inlet airflow rate and the bubbling orifice size (the description of Fuchs' theory, modified by Pich and Schütz [10], is detailed in Appendix A). From each absorption coefficient, the total collection efficiency and the efficiency due to each of the single mechanisms can be calculated and plotted for a given bubble diameter (d_b) and liquid height (h) and for each particle size (Fig. 1). Because each of these mechanisms is most effective in a given size range, the collection by a rising bubble presents a particle size that leads to a minimum efficiency (Most Penetrating Particle Size) in the range 100–500 nm.

Briefly, the collection of particles in bubble columns has been studied by several authors but most of these studies have focused on the collection of coarse and micron-sized particles. Finally, only Hermeling and Weber [8], in a short paper, focused on collection of nanoparticles. However, these collection efficiencies have been calculated from mean particle diameters and they did not mention the size distribution of generated particles. Consequently, it is difficult to definitively conclude on the influence of the particle diameter and on the mechanisms responsible for the collection of nanoparticles in a bubble rising through a liquid. Consequently, results fail to verify the separation efficiency of bubble columns towards these ultrafine particles.

3. Experimental set-up

Our study aims to determine the performance of a bubble column for nanoparticles collection. The test bench, dedicated to the study and presented below (Fig. 2), is divided into 3 main parts:

- The generation of nanoparticles is performed using a PALAS® GFG 1000 generator, operated by electric discharges in an argon

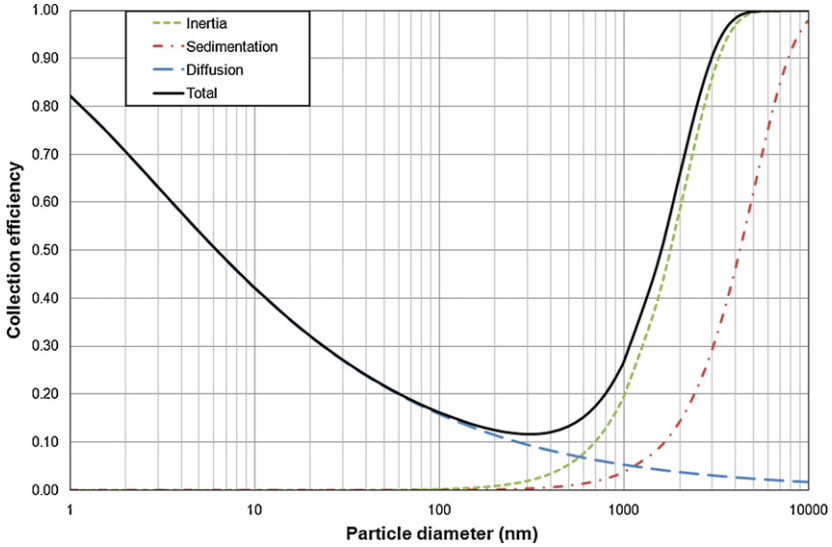

Fig. 1. Collection efficiency calculated with the Pich's model (h = 20 cm; d_b = 4 mm).

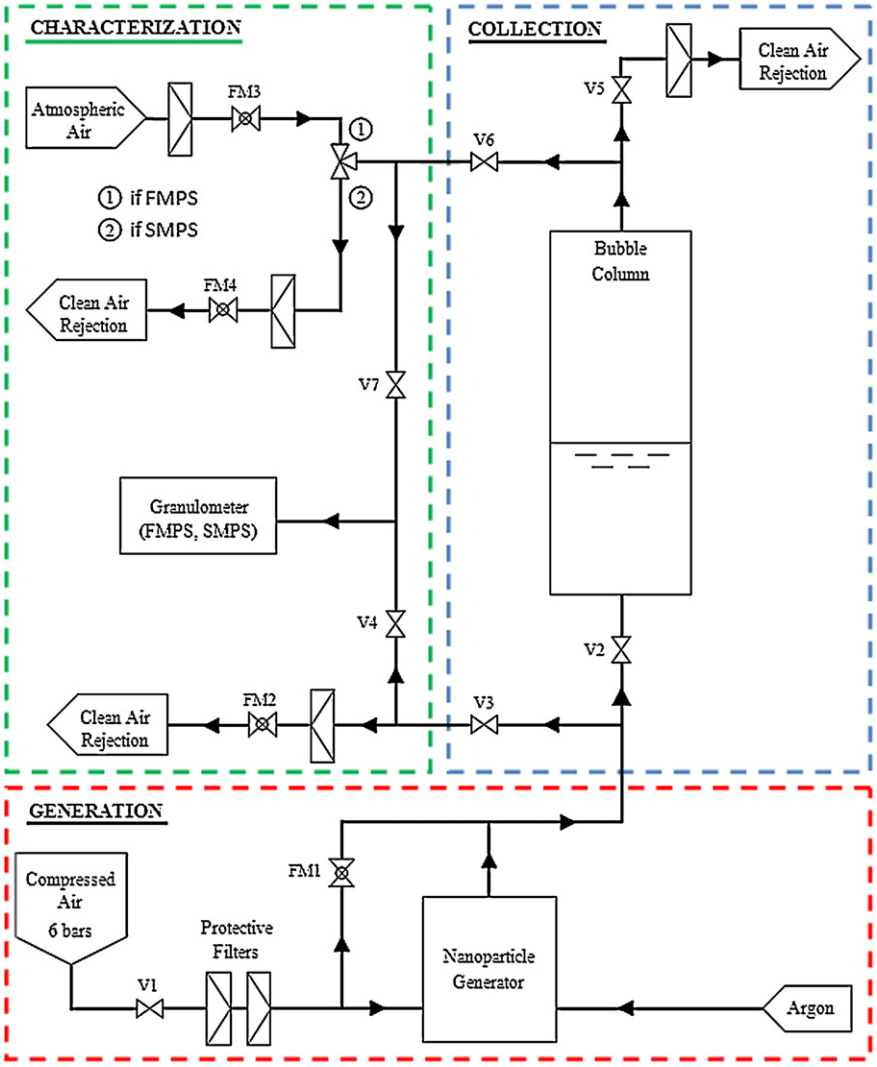

Fig. 2. Schematic view of the experimental set-up.

stream. This generation system can produce polydisperse solid particles with diameters ranging between 5 and 150 nm (Fig. 3).

- The characterization of the particle size distribution is performed upstream and downstream of the column with either a TSI® Fast Mobility Particle Sizer (FMPS) or a TSI® Scanning Mobility Particle Sizer, which both measure the electrical mobility diameter of nanoparticles. Contrary to a SMPS which associates a Condensation Particle Counter (CPC) with a Differential Mobility Analyzer (DMA), a FMPS spectrometer uses multiple, low-noise electrometers for particle detection and operates at a high flow rate (10 L/min) in order to minimize diffusion losses of ultrafine particles. For each particle size, the collection efficiency is determined from these concentration measurements upstream and downstream of the bubble column.
- The collection of nanoparticles takes place in the bubble column whose main characteristics (liquid height, bubble diameter, air flow at the column inlet) can be controlled.

An experimental study was conducted to determine the performance of a bubble column in terms of capture efficiency of carbon nanoparticles. Bubble formation occurs thanks to a perforated stainless steel plate (70 mm in diameter) with 12 orifices. The choice of demineralised water as collection fluid was done in order to avoid the formation of secondary solid particles when bubbles explode at the liquid surface. The collection efficiency of nanoparticles has been determined for liquid heights ranging from 5 to 30 cm, for various orifice diameters (330, 440 and 500 μm) and for different flows of air laden with nanoparticles (between 1 and 8 L/min). Air flow rates are always expressed at a temperature of 273 K and a pressure of 101,325 Pa.

By setting the mass flow controller FM1, it is possible to adjust the particle concentration at the inlet of the bubble column. The opening of the valves V2 and V3 allows to adjust the airflow injected into the column. The mass flow controller FM2 allows to know the bypassed flow and thus to determine the flow injected into the column by balance. This airflow entering the column can also be measured with the mass flow controller FM4 (V5 and V7 closed). To determine the particle concentration upstream of the bubble column, the valve V4 is opened so that the particle sizer (SMPS or FMPS) can pump a suitable flow. Downstream of the column, the valve V6 is closed and the air is filtered before being released into the room. For the determination of the downstream concentration, the valve V5 is closed and valve V6 is opened. But, when the FMPS granulometer is used, the suction flow is higher than the flow in the column and a previously filtered air must be pumped outside. The flowmeter FM3 allows to determine the dilution of the downstream effluent and therefore going back to its concentration. In order to overcome the eventual collection of nanoparticles on the

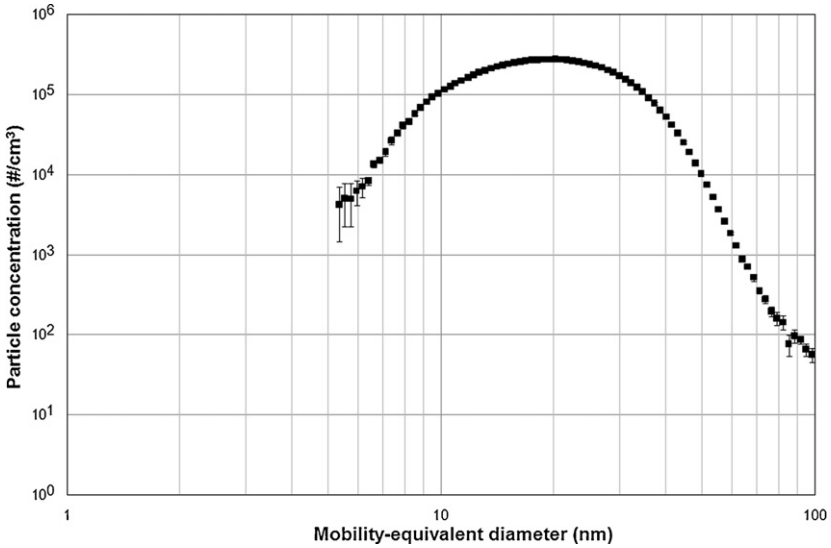

Fig. 3. Size distribution of carbon particles generated by the PALAS® GFG 1000.

walls of the column or in the pipes upstream and downstream of the column, the initial concentration, C_0, used to determine collection efficiency, is measured downstream of the column, without liquid.

It is important to note that visual observations show that the bubbling regime is homogeneous at the 12 orifices for a gas flow rate of approximately 1 L/min. Indeed, the bubbles are almost uniformly distributed and they rise uniformly through the column, without interaction between each other. At higher gas flow rates, the homogeneous gas-in-liquid dispersion cannot be maintained and an unsteady flow pattern with channelling occurs [11]. Instead of single bubbles forming, a jet appears at the orifice and it disintegrates at its top to form a lot of small bubbles [12].

4. Results and discussion

The aim of this study is to identify the influence of some operating parameters (liquid height, orifice diameter). Thus, experiments were conducted to test the influence of bubbling orifice diameter on the collection efficiency of ultrafine particles at a gas flow rate of 1 L/min and liquid heights of 20 and 30 cm. Concentration measurements upstream and downstream of the bubble column were performed with the FMPS spectrometer for perforated plates with 12 orifices of 330 or 440 μm (Fig. 4). This orifice diameter appears to influence the performance of the bubble column. Indeed, small orifices induce the formation of bubbles with smaller diameters as shown in the Gaddis and Vogelpohl relationship below [12]. This correlation is valid for all gas flow rates in the bubbling regime and is considered by Kulkarni and Joshi [13] as the most suitable for the estimation of the bubble size in stagnant liquids.

$$d_b = \left[\left(\frac{6 \cdot d_o \cdot \sigma}{\rho \cdot g} \right)^{4/3} + \left(\frac{81 \cdot \nu \cdot Q_o}{\pi \cdot g} \right) + \left(\frac{135 \cdot Q_o^2}{4 \cdot \pi^2 \cdot g} \right)^{4/5} \right]^{1/4} \quad (1)$$

where d_b is the bubble diameter (m), d_o the orifice diameter (m), σ the surface tension (N/m), ρ the collecting liquid density (kg/m^3), g the gravity acceleration (m/s^2), ν the liquid kinematic viscosity (m^2/s) and Q_o the gas flow rate through the bubbling orifice (m^3/s).

Thus if the bubble size decreases, the distance between ultrafine particles and the gas/liquid interface inside each bubble decreases

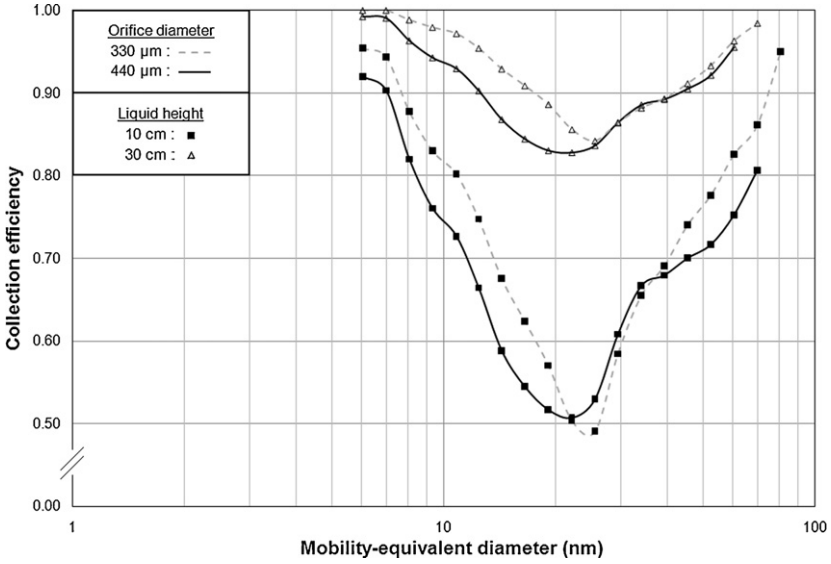

Fig. 4. Influence of orifice diameter on collection efficiency of a bubble column (Q = 1 L/min).

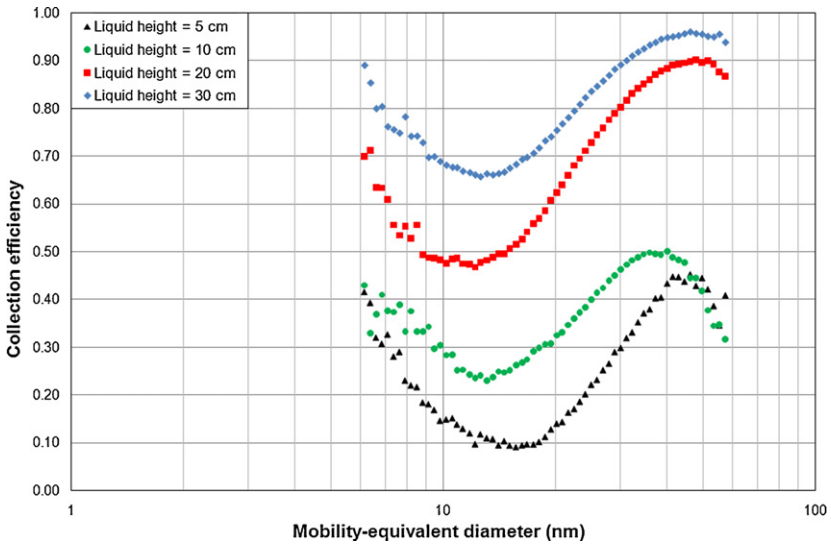

Fig. 5. Influence of liquid height on collection efficiency of a bubble column (d_o = 500 μm; Q = 5 L/min).

and the particle collection consequently increases. It is important to note that theoretical bubble diameters obtained with the correlation of Gaddis and Vogelpohl (d_b = 3.86 and 3.93 mm for orifice diameters of 330 and 440 μm; respectively) are close to experimental ones determined by visual observations and estimated at 4 mm.

Tests were also conducted in order to study the influence of the liquid height in the bubble column (Fig. 5). For a constant gas flow rate of 5 L/min and constant orifice diameters of 500 μm (this corresponds to a bubbling velocity of 35.4 m/s), the four curves obtained for different liquid heights have the same shape and highlight that the collection efficiency of nanoparticles increases with the liquid height in the column. This observation can be explained by an increase of the particles residence time in the column and thus an improvement of the particles transfer from the gas to the liquid phase.

All the experiments have also revealed the presence of a most penetrating zone for particle diameters between 10 and 30 nm. The efficiency decrease between 6 and 15 nm may be due to a decrease in collection efficiency by the diffusional mechanism and seems consistent with the modelled results of Pich and Schütz [10] (Fig. 1). In order to explain the increase in collection efficiency for particles higher than 20 nm, the presence of another mechanism has to be studied. It cannot correspond to particle sedimentation as sedimentation becomes effective only for particles higher than 200–500 nm.

This efficiency increase may be caused by electrostatic effect between charged particles. This phenomenon may contribute to the particle transport towards the gas/liquid interface of the bubble. In order to confirm this hypothesis, tests were conducted with highly positively charged carbon nanoparticles being injected in the bubble column (Fig. 6). The particle charging was performed with a charger which uses corona discharge to produce a high quantity of ions that can transfer their charge to particles passing by the charger. As a result of the charging process, particles will have a stable high positive charge state. This charging of the tested aerosol induces an increase of the collection efficiency and confirms that electrostatic effects have a real influence on the performance of a bubble column. However, this result has to be confirmed by other experiments with particles of perfectly known charge.

Figs. 5 and 6 also reveal an efficiency decrease for a particle range between 40 and 70 nm. For sake of readability, we did not represent

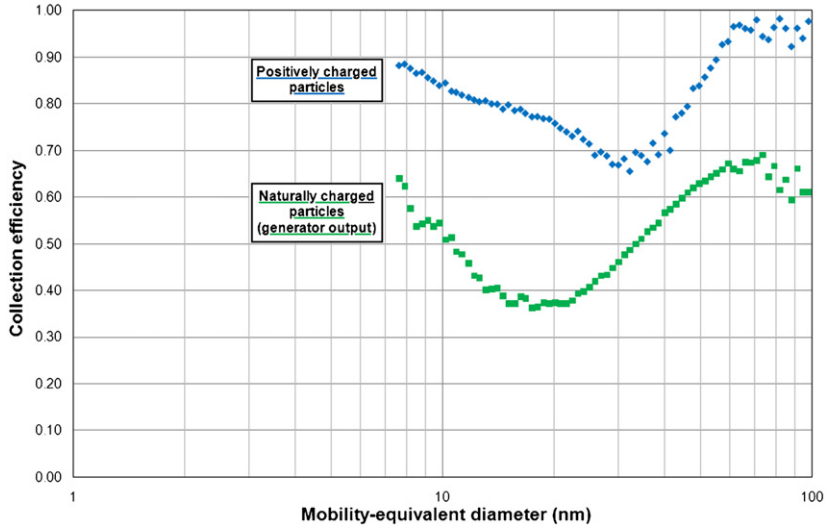

Fig. 6. Influence of particle charging on collection efficiency of a bubble column (h = 20 cm; d_o = 500 μm; Q = 3 L/min).

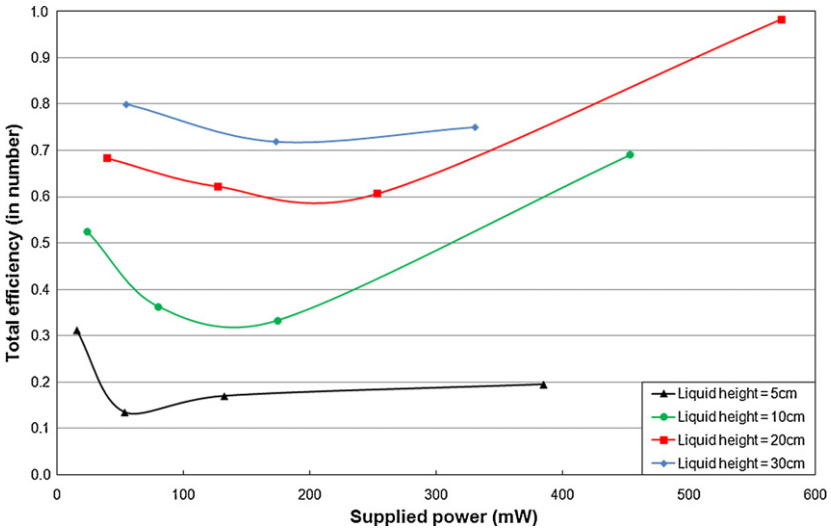

Fig. 7. Influence of the supplied power on the total collection efficiency in a bubble column.

error bars on the graphs, but for these particle sizes, collection efficiencies are subject to considerable uncertainties. Indeed, the number of particles in this size range is very low and consequently upstream and downstream measurements by the Scanning Mobility Particle Sizer are less reliable. Thus, the current results do not allow to conclude on the particle collection efficiency in a size range between 40 and 70 nm. Additional experiments with less fine aerosols may be performed in order to remove these uncertainties.

Calculations of the total collection efficiency (in number) in other operating conditions confirm conclusions on the influence of liquid height (Table 1). These data also highlight an influence of the flow of air laden with nanoparticles and this influence seems to depend on the bubbling regime. In a jetting regime (between 3 and 8 L/min), the total collection efficiency seems to increase with the airflow despite a decrease of the residence time of the air in the bubble column. Visualizations of images acquired with a fast readout camera show that a high airflow rate induces the formation and the re-entrainment of micro-bubbles in the bottom of the column. This size decrease of some bubbles and the increase of their residence time (by the re-entrainment) may explain the increase of collection efficiency at high airflows.

Pressure drop measurements were carried out during the various tests. These values are higher than those typically generated by a fibrous media but are not excessive and will not increase over time as that of a fibrous filter during its clogging. From the data of pressure drop and using Eq. (2), we calculated the power supplied during each test and compared this parameter with the total efficiency for each operating condition (Fig. 7).

$$P = Q \cdot \Delta P \tag{2}$$

where P is supplied power (W), Q the gas flow rate entering the bubble column (m^3/s) and ΔP the pressure drop between the entry and the output of the bubble column (Pa).

Table 1
Total collection efficiency for various operating conditions (d_o = 500 μm).

Total efficiency (in number)		Air flow rate			
		1 L/min	3 L/min	5 L/min	8 L/min
Liquid height	5 cm	0.312	0.135	0.170	0.195
	10 cm	0.524	0.362	0.333	0.690
	20 cm	0.683	0.622	0.606	0.982
	30 cm	0.799	0.719	0.750	–

Fig. 7 shows an efficiency minimum for low supplied powers due to the modification of the bubbling regime. In a jetting regime (between 3 and 8 L/min), the collection efficiency of nanoparticles increases with the power supplied to the system.

In the development of a new method for nanoparticles separation, energy aspects and collection efficiency must be taken into account. Consequently, the best operating conditions seem to be low airflow rates and high water levels.

5. Collection modelling in diffusional regime

Fig. 8 highlights that the bubble size greatly affects the theoretical collection efficiency. Despite the order of magnitude seems to be accurate, Pich's model underestimates experimental collection efficiencies in diffusional regime (for a bubble diameter of 4 mm which corresponds to experimental bubble diameter). Moreover, for particles smaller than 15 nm, the shape of the theoretical collection efficiency curve does not fit experimental results. Consequently, we propose a different approach from Pich's one (described previously) in order to model the particle collection by Brownian diffusion inside bubbles.

5.1. Hypotheses

- The particle concentration and the particle size distribution in each bubble are considered to be similar to measurements upstream of the column.
- Bubbles are supposed to be spherical.
- Each particle size is supposed to be homogeneously distributed in each bubble.

5.2. Calculation

Knowing the fractional particle concentration ($C_{p,j}$) in each bubble of diameter $d_{b,i}$, it is possible to determine the number of particles (of each diameter $d_{p,j}$) initially present inside a bubble.

$$N_{p,j,i,0} = \frac{\pi \cdot d_{b,i}^3}{6} \cdot C_{p,j} \tag{3}$$

By calculating the Brownian diffusion coefficient for each particle size $D_{B,j}$, the root-mean-square net displacement (l_j) of a particle

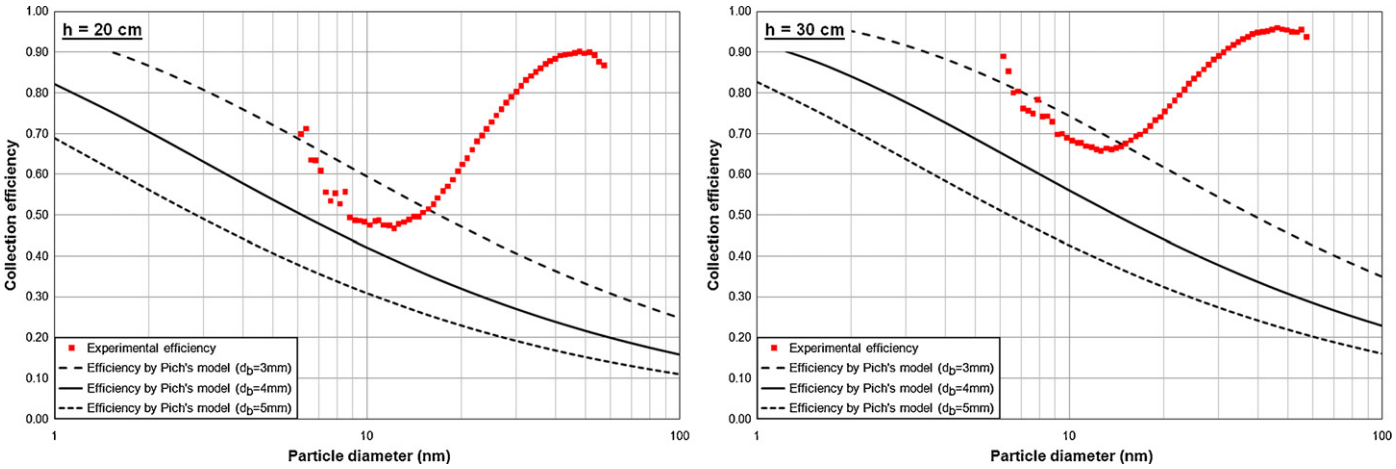

Fig. 8. Comparison between experimental data and Pich's model results.

(inside a bubble) during a time $t_{s,b}$ (which corresponds to the bubble residence time in the bubble column) can be evaluated.

$$l_j = \sqrt{2 \cdot D_{B,j} \cdot t_{s,b}} \tag{4}$$

where

$$D_{B,j} = \frac{k_B \cdot T \cdot Cu}{3 \cdot \pi \cdot \mu_G \cdot d_{p,j}} \tag{5}$$

$$t_{s,b} = \frac{h_{\text{liq}}}{U_b} \tag{6}$$

where k_B is the Boltzmann's constant (J/K), T the gas temperature (K), Cu the Cunningham correction factor, μ_G the dynamic viscosity of the gas (Pa s), h_{liq} the liquid height (m) and U_b the bubble rise velocity calculated with Eq. (A.7) (m/s).

We assume that if the Brownian displacement of a particle during the bubble time residence is higher than the bubble radius, the considered particle is collected by the liquid. The particles remaining ($N_{p,j,i,f}$) in the bubble at the end of the time $t_{s,b}$ are those which were initially at a distance from the interface higher than l_j, i.e. in the sphere of radius ($r_{b,i} - l_j$).

$$N_{p,j,i,f} = \frac{4}{3} \cdot \pi \cdot \left(\frac{d_{b,i}}{2} - l_j \right)^3 \cdot C_{p,j} \tag{7}$$

Thus we are able to determine the collection efficiency by Brownian diffusion:

$$\eta_D = \frac{N_{p,j,i,0} - N_{p,j,i,f}}{N_{p,j,i,0}} \tag{8}$$

5.3. Comparison between experimental and theoretical results

Results obtained with our modelling in the diffusional regime (for different bubble sizes) were compared with our experimental data for liquid heights of 20 and 30 cm (Fig. 9). Our theoretical and experimental collection efficiencies are in good agreement in the diffusional regime (for particles finer than 15 nm) and for bubble size of 4 mm which is close to our visual observations. The curves shape of the present model is especially closer to experimental data than with Pich's model. Nevertheless, the modelling of the collection efficiency by Brownian diffusion may be improved by a more precise determination of the experimental bubble size and by taking into account the imperfect spherical shape of the bubbles. Moreover, the modelling may be extended to other collection mechanisms (and not only Brownian diffusion) in order to confirm or infirm electrostatic effects and to explain the collection efficiency increase for particles higher than 20 nm.

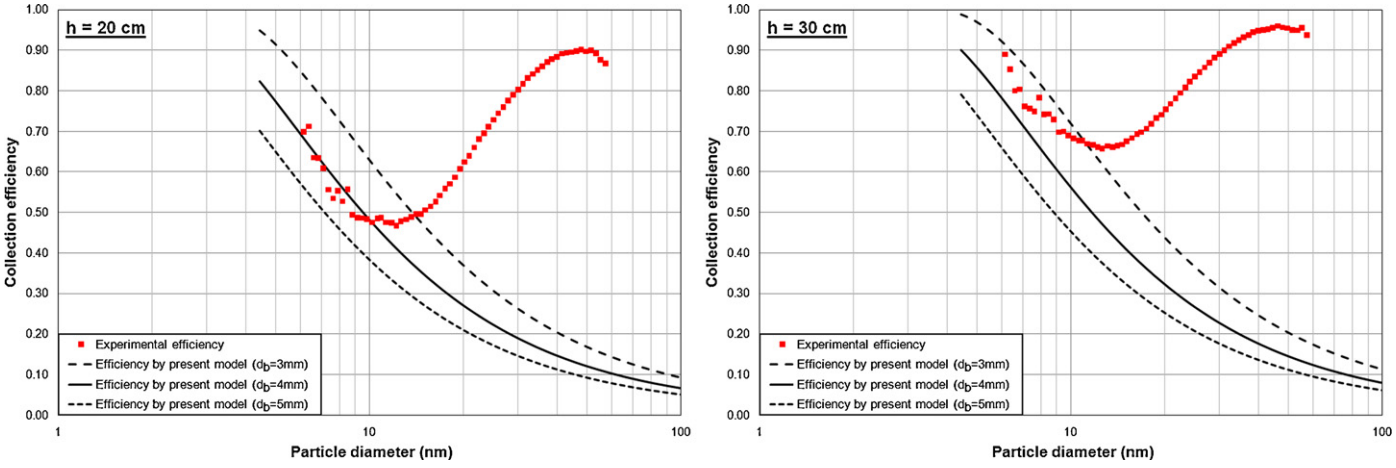

Fig. 9. Comparison between experimental data and present model results.

6. Conclusion

Despite collection efficiencies lower than those of fibrous filters, the results of this exploratory study show that the bubble columns present likely performances. An optimization of operating parameters (bubble diameter, liquid height, gas flow rate, etc.) could soon bring this technique to become a viable alternative to fibrous media in terms of collection efficiency and energy consumption. Other experiments, with particles previously neutralized or charged may also be performed in order to confirm electrostatic effects, the influence of the initial particle charge and the influence of the interactions between charged nanoparticles on collection efficiency. A more complete numerical analysis must be also developed in order to highlight the influence of the different collection mechanisms in a bubble column and to verify assumptions based on experimental results. Finally, the development of a bubble column capable of treating several hundred cubic meters per hour is also being studied in order to verify the relevance (in terms of energy expenditure and collection efficiency) of this separation process on an industrial scale.

Acknowledgments

Authors are grateful with the French National Research and Safety Institute (INRS) for its technical and financial assistance and with the French Environment and Energy Management Agency (ADEME) for the financial support of our project (agreement no. 11-81-C0084).

Appendix A. Appendix A

Deposition of aerosols in a rising gas bubble is described by the differential equation:

$$\frac{dC_p}{dh} = -a \cdot C_p \tag{A.1}$$

where C_p is the particle concentration inside the bubble, h the liquid height in the bubble column and a the absorption coefficient of particles. After integration, the previous equation becomes:

$$C_p = C_{p,0} \cdot e^{-a \cdot h} \tag{A.2}$$

where $C_{p,0}$ is the initial particle concentration inside the bubble. The total collection efficiency can be defined as:

$$\eta = 1 - \frac{C_p}{C_{p,0}} = 1 - e^{-a \cdot h} \tag{A.3}$$

Consequently, the particle collection exclusively depends on the absorption coefficient which is function of the intensity of the individual deposition mechanisms. Fuchs [9] proposed three different absorption coefficients for three deposition mechanisms: sedimentation, inertia and diffusion respectively:

$$a_S = \frac{3 \cdot g \cdot \tau}{4 \cdot U_b \cdot r_b} \tag{A.4}$$

$$a_I = \frac{9 \cdot U_b \cdot \tau}{2 \cdot r_b^2} \tag{A.5}$$

$$a_D = 1.8 \cdot \left(\frac{D_B}{U_b \cdot r_b^3} \right)^{1/2} \tag{A.6}$$

where g is gravity acceleration (m^2/s), τ the relaxation time of the particle (s), U_b the bubble rising velocity (m/s), r_b the bubble radius (m) and D_B the particle diffusion coefficient (m^2/s).

Pich and Schütz [10] used a bubble rising velocity that only depends on the bubble volume (V_b). The authors considered spherical bubbles and define an expression for the bubble rising velocity which can be included in the above equations:

$$U_b = 2.4 \cdot V_b^{1/6} = 2.4 \cdot r_b^{1/2} \cdot \left(\frac{4 \cdot \pi}{3} \right)^{1/6} \tag{A.7}$$

The particle relaxation time and the particle diffusion coefficient which appear in previous equations can be expressed as:

$$\tau = \frac{m}{6 \cdot \pi \cdot \mu_G \cdot r_p} = \frac{2 \cdot \rho_p \cdot r_p^2}{9 \cdot \mu_G} \tag{A.8}$$

$$D_B = \frac{k_B \cdot T}{6 \cdot \pi \cdot \mu_G \cdot r_p} \tag{A.9}$$

where m, ρ_p and r_p are the particle mass (kg), density (kg/m^3) and radius (m), respectively, μ_G the gas dynamic viscosity (Pa s), k_B the Boltzmann's constant (J/K) and T the gas temperature (K).

Thus, by substituting Eqs. (A.7), (A.8) and (A.9) into Eqs. (A.4), (A.5) and (A.6), expressions of absorption coefficients for the three deposition mechanisms become:

$$a_S = \frac{3^{1/6} \cdot \rho_p \cdot g}{2.4 \cdot (4\pi)^{1/6} \cdot 6 \cdot \mu_G \cdot r_b^{3/2}} \cdot r_p^2 = C_S \cdot r_p^2 \tag{A.10}$$

$$a_I = \frac{2.4 \cdot \rho_p \cdot (4\pi)^{1/6}}{3^{1/6} \cdot \mu_G \cdot r_b^{3/2}} \cdot r_p^2 = C_I \cdot r_p^2 \tag{A.11}$$

$$a_D = \frac{1.8 \cdot 3^{1/12} \cdot (k_B \cdot T)^{1/2}}{(4\pi)^{1/12} \cdot (6\pi)^{1/2} \cdot 2.4^{1/2} \cdot \mu_G^{1/2} \cdot r_b^{7/4}} \cdot \frac{1}{r_p^{1/2}} = C_D \cdot r_p^{-1/2} \tag{A.12}$$

Supposing independence and consequently additivity of the three collection mechanisms, the total absorption coefficient becomes:

$$a = (C_I + C_S) \cdot r_p^2 + C_D \cdot r_p^{-1/2} \tag{A.13}$$

References

[1] D. Bémer, R. Régnier, I. Subra, B. Sutter, M.-T. Lecler, Y. Morele, Ultrafine particles emitted by flame and electric arc guns for thermal spraying of metals, Ann. Occup. Hyg. 54 (2010) 607–614.
[2] X. Simon, D. Bémer, S. Chazelet, D. Thomas, R. Régnier, Consequences of high transitory airflows generated by segmented pulse-jet cleaning of dust collector filter bags, Powder Technol. 201 (2010) 37–48.
[3] J. Binnig, J. Meyer, G. Kasper, Origin and mechanisms of dust emission from pulse-jet cleaned filter media, Powder Technol. 25 (2009) 108–114.
[4] G. Mouret, D. Thomas, S. Chazelet, J.-C. Appert-Collin, D. Bémer, Penetration of nanoparticles through fibrous filters perforated with defined pinholes, J. Aerosol Sci. 40 (2009) 762–775.
[5] B.C. Meikap, M.N. Biswas, Fly-ash removal efficiency in a modified multi-stage bubble column scrubber, Sep. Purif. Technol. 36 (2004) 177–190.
[6] A. Bandyopadhyay, M.N. Biswas, Particulate-laden-SO_2 scrubbing in a tapered bubble column, Environ. Prog. Sustainable Energy 28 (2009) 212–225.
[7] S. Yuu, T. Yotaki, K. Abe, Investigation of the collection mechanism in absorption of aerosols by bubbling through water, Powder Technol. 17 (1977) 115–122.
[8] M. Hermeling, A.P. Weber, Nanoparticle separation from rising bubbles in aqueous solutions, in: Proceedings of World Congress on Particle Technology, Nuremberg, Germany, 2010.
[9] N.A. Fuchs, The Mechanics of Aerosols, Pergamon Press, 1964.
[10] J. Pich, W. Schütz, On the theory of particle deposition in rising gas bubbles: the absorption minimum, J. Aerosol Sci. 22 (1991) 267–272.
[11] G. Hébrard, D. Bastoul, M. Roustan, Influence of gas sparger on the hydrodynamic behaviour of bubble columns, Chem. Eng. Res. Des. 74 (1996) 406–414.
[12] E. Gaddis, A. Vogelpohl, Bubble formation in quiescent liquids under constant flow conditions, Chem. Eng. Sci. 41 (1986) 97–105.
[13] A.A. Kulkarni, J.B. Joshi, Bubble formation and bubble rise velocity in gas-liquid systems: a review, Ind. Eng. Chem. Res. 44 (2005) 5473–5931.